Scanning tunneling microscopy studies of the $Fe_3O_4(001)$ surface using antiferromagnetic probes

G. Mariotto,[a] S. F. Ceballos, S. Murphy, and I. V. Shvets
SFI Laboratories, Physics Department, Trinity College, Dublin 2, Ireland

(Presented on 13 November 2002)

We have studied the (001) surface of a Fe_3O_4 single crystal using low-energy electron diffraction (LEED), Auger electron spectroscopy (AES) and scanning tunneling microscopy (STM). The STM measurements were performed using a novel tip of antiferromagnetic MnNi alloy. Atomically resolved STM images provide evidence of a surface terminated at the octahedral plane, with rows of Fe cations running along the $\langle 110 \rangle$ crystallographic axes. Two different kinds of Fe cations with a separation of 6 Å were imaged, while the periodicity between Fe cations of the same kind is about 12 Å. We propose an interpretation of the anomalous corrugation observed in terms of a spin polarized effect, resulting in magnetic contrast between Fe^{2+} and Fe^{3+} ions in octahedral coordination. © *2003 American Institute of Physics.* [DOI: 10.1063/1.1556199]

I. INTRODUCTION

Scanning tunneling microscopy (STM) has proven to be a powerful instrument for the investigation of the structure and electronic properties of surfaces down to the nanometer and atomic scale. In recent years, attention has focused on the possibility of obtaining magnetic contrast by using STM with tips made from magnetic materials. Magnetic contrast on the atomic scale was claimed by Wiesendanger *et al.*[1] on the $Fe_3O_4(001)$ surface of a natural single crystal using a ferromagnetic Fe tip. These results were recently reproduced by Koltun *et al.*[2] on an artificial $Fe_3O_4(001)$ single crystal. Cr coated W tips have also been employed to image stripe domains with a magnetic period of 50 ± 5 nm in Fe/W(110) epitaxial films.[3] Antiferromagnetic tips do not produce a stray magnetic field, so that there should be no magnetostatic interaction between the tip and sample.[4] In this study, we fabricated tips from antiferromagnetic MnNi and used them to investigate the surface properties of magnetite, $Fe_3O_4(001)$. Magnetite is a highly interesting material for applications in spin electronics, because of its half-metallic properties. However, many issues regarding the structural and electronic properties of the surface have not been resolved. In this study, new STM data are presented on the structure of the (001) surface at the atomic scale. These results are discussed in terms of a possible spin-polarized effect.

II. EXPERIMENT

The sample preparation and analysis were performed in an UHV system with a base pressure in the mid 10^{-11} mbar. This system was equipped with facilities for low-energy electron diffraction (LEED) and Auger electron spectroscopy (AES). STM was performed in constant-current mode, using a home-built room-temperature instrument. The sample was positively biased at 0.6–1.0 V with respect to the tip. A tunneling current between 0.1 and 0.3 nA was typically used.

Magnetite is an inverse spinel material with a crystal structure that is based on a face-centered cubic unit cell, containing 32 O^{2-} anions and 24 mixed valence Fe cations, having a lattice parameter of $a = 8.3963$ Å.[5] The formula can be written as $Y_A[XY]_BO_4$, where $X = Fe^{2+}$, $Y = Fe^{3+}$ and A and B denote tetrahedral and octahedral sites, respectively. The octahedral B sites are occupied by a mixture of Fe^{2+} and Fe^{3+} ions, which form rows running along the $\langle 110 \rangle$ set of directions. Magnetite is a half-metallic ferrimagnet with a high spin-polarization near the Fermi level.[6] The spin configuration of the Fe ions is $3d^5$ for Fe^{3+} and $3d^6$ for Fe^{2+}, making the (001) face terminated at the octahedral plane suitable for atomic scale spin-polarized STM experiments.

The artificial crystal used in these experiments was grown by the skull melting technique.[7] The crystal surface was aligned with a precision of $\pm 1°$ with respect to the (001) crystallographic plane. X-ray diffractometry (XRD) of a powdered part of the crystal showed good agreement with the reference diffractograms for the magnetite crystal structure and a lattice constant of 8.40 ± 0.01 Å was measured. Four-point resistance versus temperature measurements were made between 10 and 300 K. A Verwey transition temperature of 108 K was measured, indicating that the composition of the crystal was substoichiometric.

The crystal was mechanically polished using diamond paste with decreasing grain sizes of 3, 1, and 0.25 μm. After polishing, the crystal was cleaned and secured onto a Mo sample holder before insertion into the UHV system. The in-vacuum preparation procedure consisted of a combination of Ar^+ ion sputtering, annealing in UHV, and annealing in an oxygen partial pressure. The details of this preparation procedure are described elsewhere.[8] This preparation procedure produces a contaminant-free surface, showing a sharp $(\sqrt{2} \times \sqrt{2})R45°$ LEED pattern.

[a]Electronic mail: mariotl@tcd.ie

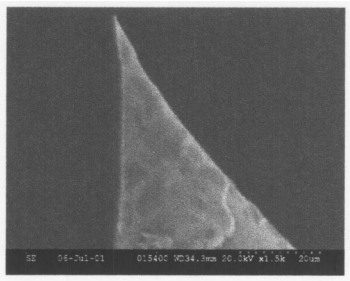

FIG. 1. SEM images of a MnNi tip with ×1.5k magnification.

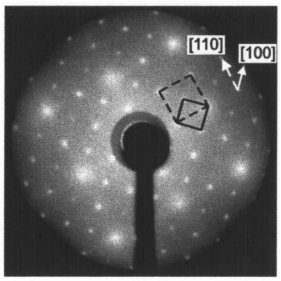

FIG. 2. LEED pattern of a clean $Fe_3O_4(001)$ surface observed with a primary electron energy of 93 eV. The $(\sqrt{2}\times\sqrt{2})R45°$ surface mesh is visible. The $p(1\times1)$ unit cell and the $(\sqrt{2}\times\sqrt{2})R45°$ superlattice are indicated by a dashed square and a solid square, respectively. The crystallographic axes are marked.

III. RESULTS AND DISCUSSION

A. Tips fabrication

STM tips for this study were fabricated using MnNi alloy. The MnNi alloy has a CuAu–I type face centered tetragonal crystal structure, with lattice parameters $a=3.714$ Å, $c=3.524$ Å. This alloy is antiferromagnetic within a composition range of about ±2% of the equiatomic composition.[9] Neutron diffraction studies indicate that the Mn atoms have large magnetic moments ($\mu=4.0\pm0.1\mu_B$), which are antiferromagnetically aligned in planes that are normal to the crystallographic c axis. The magnetic moments of the Ni atoms are by comparison much smaller ($\mu\leqslant0.6\mu_B$).[10,11]

A polycrystalline ingot was prepared by arc-melting equiatomic proportions of 99.9% pure Mn and Ni powder under an argon atmosphere. Having melted the ingot twice to ensure homogeneity, it was then annealed for 48 h at 900 °C under an inert argon atmosphere. X-ray powder diffraction was carried out on a sample of the ingot to ensure that the correct crystallographic structure was obtained. Cylindrical rods (0.5 mm×13 mm) of the material were then prepared by cutting the ingot with a low-speed diamond-wheel saw and polishing.

We have employed a similar technique to that described by Iijima and Yasuda[12] for the preparation of Fe, Ni, and FeBSiC magnetic force microscope (MFM) tips. The MnNi rods were etched in an aqueous solution of 0.5 M HCl. The lower end of each rod was covered with a length of 2.5 mm of insulating PTFE tubing, which was then immersed in the etchant. This physically restricted the etching zone because only a very small region of the uncovered rod above the insulating tubing was exposed to the etchant. Dropoff occurred when the etched region was too narrow to support the weight of the lower portion of the rod. The tip was retrieved from the PTFE tubing which protected it from mechanical damage after dropoff. The tips were rinsed with distilled water and inserted into the UHV system where they were cleaned with 1 keV Ar^+ ions prior to use. This technique improves upon earlier preparation procedures developed in our laboratory,[13,14] to produce tips with a lower aspect ratio and with tip apexes lying in the 50–100 nm range. SEM images of a MnNi tip prepared in this fashion are shown in Fig. 1. A more detailed description of the tips preparation procedure is available elsewhere.[15]

B. AES and LEED measurements of $Fe_3O_4(001)$

The Fe–O system is complex and the stable phases depend on parameters such as temperature and oxygen content. Fe_3O_4, FeO, and γ-Fe_2O_3 have a similar oxygen lattice and can readily transform into each other under suitable anneal conditions. Therefore, it is important to establish which phase may be present on the surface of a crystal. AES can be used to establish the chemical composition of the surface; the Fe $M_{2,3}VV$ line shape can be used to determine which iron oxide is present at the surface.[16–19] The typical line shape of the low-energy iron peaks we obtained are in good agreement with the reference Auger spectrum for Fe_3O_4.[17] This line shape was found to be highly reproducible using the in-vacuum preparation procedure described earlier. Figure 2 shows a typical LEED pattern of the surface, taken with a primary beam energy of 93 eV and an emission current of 0.5 mA. Half-order spots are visible in an arrangement corresponding to a $(\sqrt{2}\times\sqrt{2})R45°$ reconstruction. The (1×1) unit cell and the $(\sqrt{2}\times\sqrt{2})R45°$ superlattice are indicated by a dashed and a solid square, respectively.

C. STM measurements of $Fe_3O_4(001)$

A typical STM image of the surface is shown in Fig. 3. The (001) surface of magnetite was characterized by flat terraces with straight edges aligned along the [110] and [1$\bar{1}$0] crystallographic directions. The step heights are an integer multiple of 2.1 Å, which corresponds to the separation between $A-A$ or $B-B$ planes. A monatomic step equal to 1.0

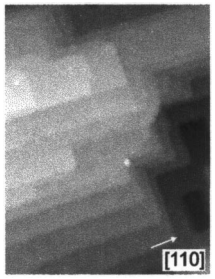

FIG. 3. (1200×1500) Å^2 STM image. The step edge directions lie along the [110] and [1$\bar{1}$0] crystallographic axes. The step heights are integer multiple of 2.1 Å, which corresponds to the separation between $A-A$ or $B-B$ planes.

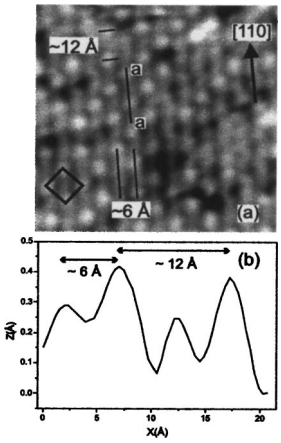

FIG. 4. (a) (70×70) Å^2 STM image. An ~6 Å distance between neighboring rows is observed. The image was acquired at a positive sample bias of 1.0 V and a tunneling current of 0.1 nA using a MnNi tip; (b) line profile taken along the line $a-a$. The separation between two points of enhanced corrugation along the ⟨110⟩ directions is ~12 Å; a point of lesser corrugation, at an equal distance of ~6 Å between two points of enhanced corrugation is revealed by the line profile.

±0.1 Å was never observed, ruling out the possibility of both tetrahedral and octahedral atomic planes coexisting on the clean surface. Higher resolution zooms reveal an atomic structure, as shown in Fig. 4(a). The atomic rows run along the [110] crystallographic axis and are separated by ~6 Å. A comparison of atomically resolved images with structures corresponding to possible *A* and *B* plane terminations revealed that the surface, containing an alternating corrugation along the [110]-oriented atomic rows, consists of *B*-terminated terraces. This result is in agreement with our earlier STM results of $Fe_3O_4(001)$ using nonmagnetic tips, where a twofold symmetry, corresponding to the octahedral plane, was observed.[20]

Closer inspection of these rows reveals that the corrugation along each row alternates between points of enhanced corrugation and points of lesser corrugation, as shown by the line profile labeled $a-a$ in Fig. 4(b). The periodicity of the rows along the [110] direction is ~12 Å between points of similar corrugation, and 6 Å between points of different corrugation. A 3 Å periodicity, as expected for octahedral Fe in bulk magnetite, has not been observed. The periodicity along the [100] direction is ~8.4 Å, in agreement with the value measured from the LEED pattern in Fig. 2. A cubic symmetry is clearly seen on the surface; a black square marked in Fig. 4(a) can be identified with the $(\sqrt{2}\times\sqrt{2})R45°$ reconstructed unit cell seen in the LEED pattern (Fig. 2).

For STM imaging, both theoretical calculations[6] and experimental evidence[21] have indicated that the O $2p$ states lie well below E_F and are therefore not accessible for tunneling experiments. As a result, we conclude that STM images of Fe_3O_4 are obtained by probing the Fe cation states, which form the corrugation along the atomic rows on the surface in Fig. 4(a).

As indicated earlier, the octahedrally terminated $Fe_3O_4(001)$ surface is an attractive candidate for SPSTM experiments because of the different spin configuration of the Fe^{3+} and Fe^{2+} cations. Slonczewski[22,23] has shown that the tunneling conductance between two ferromagnets separated by a nonmagnetic barrier is dependent on the relative orientation of the quantization axes in both ferromagnets. Translated to a STM junction, this means that the tunneling current depends on the magnetization of the tip $\mathbf{m}_T$ and the sample $\mathbf{m}_S$. Assuming a constant tip magnetization, the variation of the tunneling current will be dependent on $\mathbf{m}_S$. Since the magnetic moments of Fe^{2+} and Fe^{3+} in magnetite are $4\mu_B$ and $5\mu_B$, respectively, these ions should be distinguishable using a spin-polarized tip. The anomalies in the atomic corrugation detected in our measurements [see Fig. 4(b)] may be the result of this spin-polarized effect. At present, this structure has not been reproduced using a nonmagnetic tip. A comparison with atomically resolved images obtained using nonmagnetic tips (e.g., W) would clarify whether a spin-polarized mechanism is definitely involved, or if a difference in the local density of states (LDOS) of Fe^{2+} and Fe^{3+} ions is responsible. A more extensive analysis of the results discussed above is available elsewhere.[24]

ACKNOWLEDGMENTS

The authors would like to thank Professor J. M. Honig for providing the magnetite crystals used in this study. Financial assistance from the Science Foundation Ireland (SFI) Agency, Contract No. 00/PI.1/C042, is gratefully acknowledged.

[1] R. Wiesendanger, I. V. Shvets, D. Bürgler, G. Tarrach, H. J. Güntherodt, J. M. D. Coey, and S. Gräser, Science **255**, 583 (1992).
[2] R. Koltun, M. Herrmann, G. Güntherodt, and V. A. M. Brabers, Appl. Phys. A: Mater. Sci. Process. **73**, 49 (2001).
[3] A. Kubetzka, M. Bode, O. Pietzsch, and R. Wiesendanger, Phys. Rev. Lett. **88**, 057201 (2002).
[4] A. Minakov and I. V. Shvets, Surf. Sci. **236**, L377 (1990).
[5] R. W. G. Wyckoff, *Crystal Structures*, 2nd ed. (1964).
[6] A. Yanase and K. Siratori, J. Phys. Soc. Jpn. **53**, 312 (1984).
[7] J. E. Keem, H. R. Harrison, R. Aragon, and J. M. Honig, Inorg. Synth. **22**, 43 (1984).
[8] G. Mariotto, S. Murphy, and I. V. Shvets (unpublished).
[9] W. Pearson, K. Brun, and A. Kjekshus, Act. Chem. Scand. **19**, 477 (1965).
[10] J. Kasper and J. Kouvel, J. Phys. Chem. Solids **11**, 231 (1959).
[11] L. Pál, E. Krén, G. Kádár, P. Szabó, and T. Tarnóczi, J. Appl. Phys. **39**, (1968).
[12] T. Iijima and K. Yasuda, J. Acoust. Soc. Jpn. **27**, 1546 (1988).
[13] S. Murphy, J. Osing, and I. V. Shvets, J. Magn. Magn. Mater. **198–199**, 686 (1999).
[14] S. Murphy, J. Osing, and I. V. Shvets, Appl. Surf. Sci. **144–145**, 497 (1999).
[15] S. Ceballos, G. Mariotto, S. Murphy, and I. V. Shvets, Surf. Sci. **131–140**, 523 (2003).
[16] M. Seo, J. B. Lumsden, and R. W. Staehle, Surf. Sci. **50**, 541 (1975).
[17] V. S. Smentkowski and J. T. Yates, Surf. Sci. **232**, 113 (1990).
[18] D. Briggs and M. P. Seah, *Practical Surface Analysis*, 2nd ed. (Wiley, New York, 1990), Vol. 1.
[19] C. Ruby, J. Fusy, and J. M. R. Genin, Thin Solid Films **352**, 22 (1999).
[20] C. Seoighe, J. Naumann, and I. V. Shvets, Surf. Sci. **440**, 116 (1999).
[21] S. F. Avarado, M. Erbudak, and P. Munz, Phys. Rev. B **14**, 2740 (1976).
[22] J. C. Slonczewski, J. Phys. C **8**, 1629 (1988).
[23] J. C. Slonczewski, Phys. Rev. B **39**, 6995 (1989).
[24] G. Mariotto, S. Murphy, and I. V. Shvets, Phys. Rev. B **66**, 245426 (2002).